Thermochimica Acta, 150 (1989) 141–152
Elsevier Science Publishers B.V., Amsterdam – Printed in The Netherlands

ORDER–DISORDER PHASE TRANSITIONS IN β-$MnSO_3$ $3H_2O$–TYPE HYDRATES: ISOTOPIC EFFECTS—VIBRATIONAL, X-RAY, THERMOANALYTICAL AND PERMITTIVITY MEASUREMENTS

J. HENNING and H.D. LUTZ

Universität Siegen, Anorganische Chemie I, Postfach 101240, D-5900 Siegen (F.R.G.)

(Received 30 January 1989)

ABSTRACT

Low-temperature phase transitions of the isomorphic $MSO_3 \cdot 3H_2O$ (M = Mg, Mn, Fe, Co, Ni, Zn, *oP*56, β-$MnSO_3 \cdot 3H_2O$-type) have been studied by IR, Raman, X-ray, DSC and dielectric constant measurements. The phase transitions occur in two successive processes: (i) freezing out of the dynamic disorder of one kind of the H_2O molecules (all compounds) and (ii) monoclinic distortion of the orthorhombic cell of the room temperature phases, which has only been demonstrated in the case of the magnesium (207 K), manganese (217 K) and cobalt (230 K) compounds. A strong decrease in the transition temperatures with increasing deuterium content is observed.

INTRODUCTION

Phase transitions in solid hydrates are often connected with disorder of the protons of the water molecules [1,2]. These order–disorder transitions are mainly of second or higher order. Structural changes with respect to the heavy atoms are mostly small and, hence, thermal analyses (DTA, DSC) and X-ray studies give little information. Vibrational spectroscopy, however, seems to be a valuable tool for studying phase transitions of order–disorder type [3,4] in solid hydrates [1,2,5]. The variation of both band frequencies and band shapes (halfwidths) of soft and hard modes with temperature can be examined in this way. Particularly, the stretching bands (both in IR and Raman) of matrix-isolated HDO molecules (isotopically dilute samples) are an excellent probe of the local potential at the proton sites and therefore are very sensitive to structural changes concerning the water molecules.

Thus, a low temperature modification (LTM) of $MgSO_3 \cdot 3H_2O$ has been found along with unexplained H/D isotopic effects by means of spectroscopic studies [6]. In this paper, the results of a detailed examination of this order–disorder transition are presented including data on isomorphic $MSO_3 \cdot 3H_2O$ compounds (M = Mn, Fe, Co, Ni, Zn), based on IR and Raman

0040-6031/89/$03.50

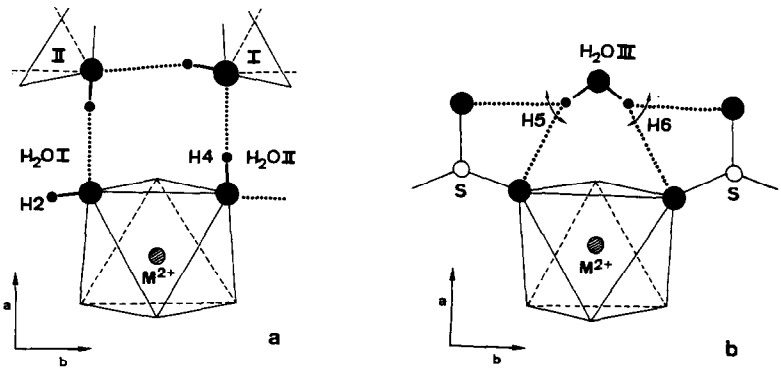

Fig. 1. Parts of the crystal structure of $MSO_3 \cdot 3H_2O$ (M = Mg, Mn) [8,9] (projections along [001]). Dotted lines, hydrogen bonds; (a), H_2O I and H_2O II, H(1) and H(3) (not shown) above and below the respective O atoms; (b), H_2O III; arrows indicate dynamic disorder.

spectroscopy, X-ray, thermoanalytical and permittivity measurements. In addition, the influence of the H/D exchange on this transition was studied.

The sulphite trihydrates of β-$MnSO_3 \cdot 3H_2O$-type [7–9] crystallize in the orthorhombic space group $P2_12_12_1$ with $Z = 4$ ($oP56$). For the monoclinic polymorphs of $MSO_3 \cdot 3H_2O$, the α-$FeSO_3 \cdot 3H_2O$-type and β-$FeSO_3 \cdot 3H_2O$-type see refs. 7 and 8. In the case of the orthorhombic compounds, there are three crystallographically different water molecules, H_2O I–III, with six different H positions in the structure (see Fig. 1). Both hydrogen atoms of H_2O III are involved in bifurcated H-bonds. They show large thermal ellipsoids, possibly due to rotational disorder of these water molecules at ambient temperature. The orientational disorder of H_2O I and II supposed in refs. 6 and 8, however, could not be confirmed by the neutron diffraction studies [9].

EXPERIMENTAL

Preparation of single crystals and polycrystalline samples

For the preparation of the orthorhombic sulphite trihydrates under discussion three techniques were used [5,7]: (i) crystallization from an aqueous $M^{II}(HSO_3)_2$ solution; (ii) gel crystallization technique with a $M^{II}Cl_2$ or $M^{II}SO_4$ solution and a Na_2SO_3 solution (both ≈ 0.5 M) placed in the two arms of a U-shaped tube above silicic acid gel; and (iii) diffusion of $M^{II}Cl_2$ or $M^{II}SO_4$ and Na_2SO_3 solutions (0.25–0.5 M) through a Na_2SO_4 or a NaCl solution (0.5–1.0 M).

Fully and partially deuterated samples were obtained by application of D_2O or H_2O/D_2O mixtures as solvents, and crystallization in N_2 or D_2O atmosphere. Details are given elsewhere [5], for $Mg(SO_3)_2 \cdot 3H_2O$ [6], β-

$MnSO_3 \cdot 3H_2O$ and $ZnSO_3 \cdot 3H_2O$ [10], γ-$FeSO_3 \cdot 3H_2O$ and $NiSO_3 \cdot 3H_2O$ [7] and $CoSO_3 \cdot 3H_2O$ [11].

Apparatus and techniques

The IR spectra of the polycrystalline samples were recorded on a Perkin–Elmer model 580 spectrophotometer (resolution < 0.5 cm^{-1}) using KBr and CsI discs as well as Nujol and Fluorolub mulls. In the case of $ZnSO_3 \cdot 3H_2O$, reaction with KBr was observed. Raman spectra, with the samples in glass capillary tubes, were measured on a Dilor OMARS 89 multichannel spectrograph (resolution < 4 cm^{-1}). For excitation the 514.5, 488.0 and 457.9 nm lines of an Ar^+ ion laser were employed using both right-angle and backscattering geometries. The integration times were 1–60 s and the number of accumulations were 20–100 (signal averaging). Low temperature spectra were recorded with the use of variable temperature cells, Coderg model CRN2 (100–300 K) and Oxford Instruments model CF 104 (10–300 K) (Raman), RIIC model VLT2 (IR). The accuracy of the temperatures given is about ± 2 K (± 5–10 K for Co, Ni and Zn compounds).

X-ray diffraction patterns in the temperature range 100–300 K were obtained with an Enraf–Nonius Guinier Simon camera (Cu $K\alpha_1$, α-SiO_2 and Si as internal standards). Unit cell dimensions were computed by a least-squares method (LSUCR). DTA (differential thermal analysis) and DSC (differential scanning calorimetry) measurements were made in a dry nitrogen stream using a Perkin–Elmer DSC 7 calorimeter. The heating rates were 10 and 20° min^{-1}; references were Al_2O_3 or empty aluminium pans. The permittivities (dielectric constants) were obtained by means of impedance measurements (Hewlett–Packard model 4192 impedance analyser) via the capacity in an AC circuit (10–100 KHz) using polycrystalline samples pressed into pellets ($4–6 \times 10^3$ Pa).

RESULTS

X-ray measurements

X-ray studies of the orthorhombic $MSO_3 \cdot 3H_2O$ (M = Mg, Mn, Fe, Ni, Zn) (temperature range 100–300 K) indicate a low-temperature phase transition in the case of the magnesium and manganese compounds at ≈ 200 and ≈ 210 K, respectively, but not for the iron, nickel or zinc compounds. (In the case of the manganese compound, this transition was only observed in two out of four experimental runs.) For $CoSO_3 \cdot 3H_2O$, no reliable X-ray data were available (fluorescence due to Cu $K\alpha_1$ radiation). The splittings of the $0kl$ and hkl reflections observed for $MgSO_3 \cdot 3H_2O$ (Fig. 2) and β-$MnSO_3 \cdot 3H_2O$ indicate a small monoclinic distortion of the orthorhombic

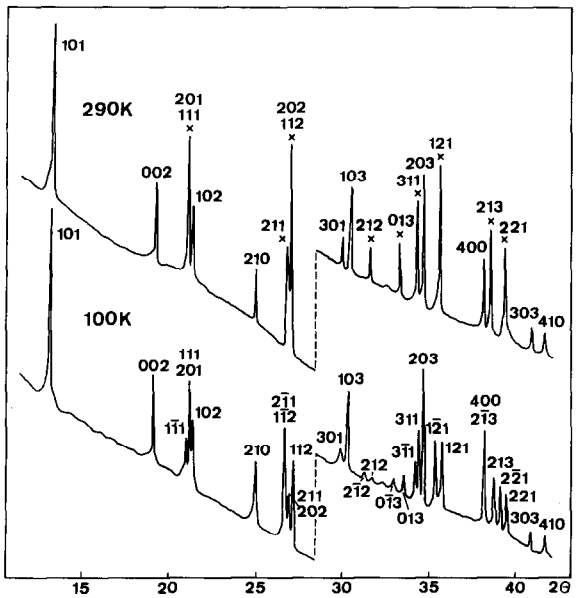

Fig. 2. X-ray Guinier powder photographs (densitometer registration) of $MgSO_3 \cdot 3H_2O$ RTM (290 K) and TTM (100 K); *x*, reflections split at low temperature.

TABLE 1

Unit cell dimensions *a*, *b*, *c*, α (pm, °) and cell volume ($10^6 \times pm^3$) of room and low temperature polymorphs of $MgSO_3 \cdot 3H_2O$ and β-$MnSO_3 \cdot 3H_2O$

		a	*b*	*c*	α	*V*	
$MgSO_3 \cdot 3H_2O$	RTM	954.5 (1)	552.1 (1)	937.7 (1)	90	494.1	[8]
	LTM	951.2 (2)	551.3 (1)	937.3 (2)	91.23 (2)	491.4	
β-$MnSO_3 \cdot 3H_2O$	RTM	976.7 (1)	563.7 (1)	956.0 (1)	90	526.4	[8]
	LTM	971.5 (4)	563.2 (2)	957.9 (3)	91.07 (3)	524.0	

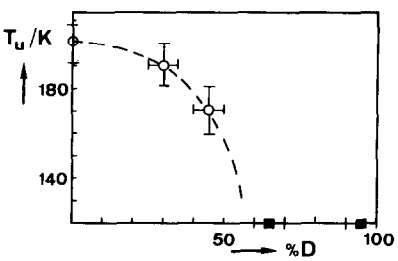

Fig. 3. Phase transition of $MgSO_3 \cdot 3H_2O$ (RTM → LTM) as a function of the deuterium content as observed by X-ray studies; ■, no phase transition down to ≈120 K.

unit cell. The probable space group of the LTM is $P2_111$ ($mP56$). Least-squares methods resulted in the lattice constants given in Table 1. $\vec{a}$, which is chosen as the unique axis for comparison with the crystal data of the room temperature polymorphs, is significantly shortened compared to the RTMs. As shown from both X-ray and vibrational data, these new $MSO_3 \cdot 3H_2O$ polymorphs are different from the monoclinic α-$FeSO_3 \cdot 3H_2O$-type and β-$FeSO_3 \cdot 3H_2O$-type hydrates [7,8].

With increasing deuterium content of the samples, a decrease in the transition temperatures is revealed from X-ray (and vibrational [6]) data (Fig. 3). Thus, in the case of the magnesium compound, specimens deuterated by more than $\approx 60\%$ do not show the LTM down to liquid nitrogen temperature.

Thermoanalyses

DTA and DSC measurements of $MgSO_3 \cdot 3H_2O$, β-$MnSO_3 \cdot 3H_2O$ and $CoSO_3 \cdot 3H_2O$ confirm the phase transitions mentioned above. They occur in the form of broad features at 207, 217 and 230 K (± 3 K, peak maxima of heating runs), respectively. However, the enthalpy changes of these reversible transitions (hysteresis ≈ 5 K) are small, i.e. ≈ 0.1 kJ mol^{-1}, particularly compared with that (162 kJ mol^{-1}) found for dehydration of $MgSO_3 \cdot 3H_2O$ at 462 K. The graphs (heat flow versus temperature) show, in addition, small baseline shifts at ≈ 225 K ($MgSO_3 \cdot 3H_2O$) and ≈ 235 K (β-$MnSO_3 \cdot 3H_2O$). For details see ref. 5.

Dielectric constants

The temperature dependence of the dielectric constant (permittivity) ($\epsilon(T)$) of polycrystalline samples of the magnesium compound is given in Fig. 4. The graph obtained is characteristic for the transition from a paraelectric to an electrically ordered material [12]. In the case of $MgSO_3 \cdot 3H_2O$, ordering takes place below ≈ 230 K, as revealed from the maximum of the ϵ versus T curve.

Vibrational spectroscopy

Phase transitions to low temperature polymorphs of the β-$MnSO_3 \cdot 3H_2O$-type compounds are clearly revealed by the IR and Raman spectra especially by those of isotopically dilute samples (deuterated for $\approx 5\%$ D), i.e. the OD modes (ν_{OD}) of matrix isolated HDO molecules (see Figs. 5–7 and [6]). In the case of the magnesium, manganese and cobalt compounds, there are clear discontinuities of the frequency shifts in the region of the transition temperatures (207, 217 and 230 K, see above), while in the spectra of the iron, nickel and zinc compounds, these changes are only small and more

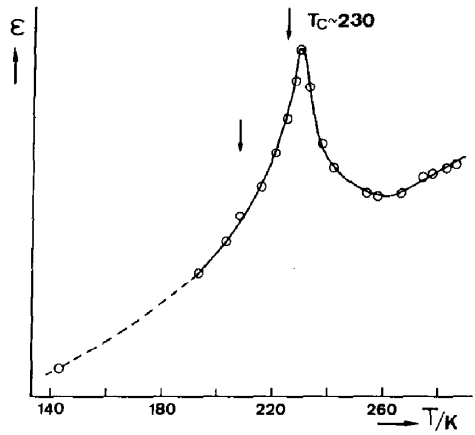

Fig. 4. Permittivity of $MgSO_3 \cdot 3H_2O$ as a function of temperature; arrows, phase transitions observed by vibrational spectroscopy and thermal analysis.

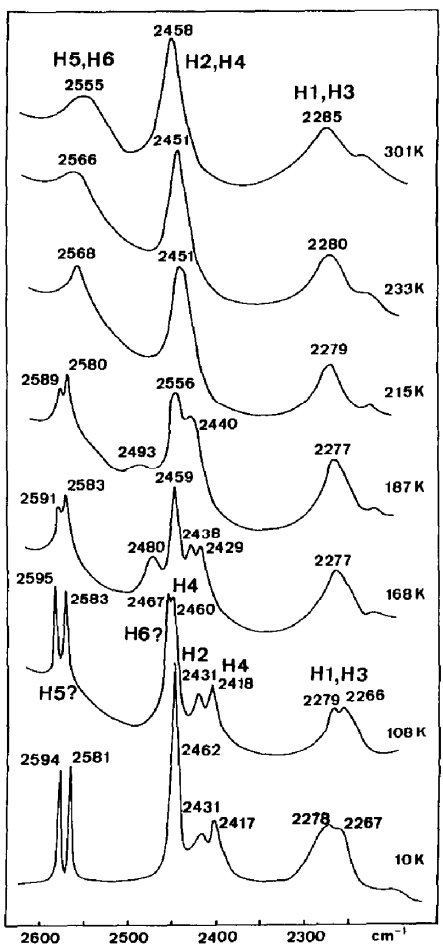

Fig. 5. Raman spectra of isotopically dilute samples of $MgSO_3 \cdot 3H_2O$ in the ν_{OD} mode region at various temperatures (for assignment see Fig. 6).

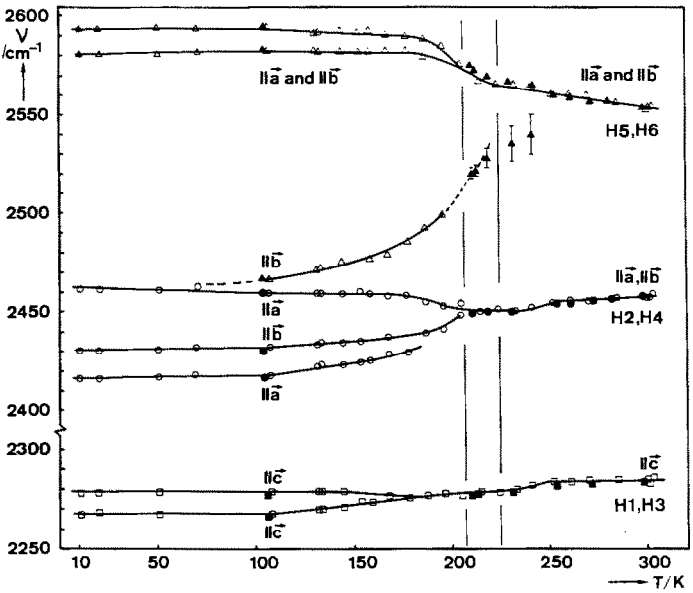

Fig. 6. Temperature dependence of the band frequencies of uncoupled OD modes (HDO molecules, isotopically dilute samples) due to the various hydrogen positions of $MgSO_3 \cdot 3H_2O$ (H1–H6, see Fig. 1). Filled signs, IR spectra; open signs, Raman data (Fig. 5); vertical lines, phase transitions; assignment of the ν_{OD} bands, i.e. alignment of the respective OD oscillator with respect to the crystal axes ($\| \vec{a}$, $\| \vec{b}$, $\| \vec{c}$), by means of Raman single crystal measurements [5,6,13].

continuous. With the exception of γ-$FeSO_3 \cdot 3H_2O$, all β-$MnSO_3 \cdot 3H_2O$-type compounds, however, exhibit more than six, and at least up to eight, OD bands in the low temperature spectra (Figs. 5–7), which means that there must be more than six different hydrogen positions in the LTMs, as found for the room temperature modification (RTM) from neutron diffraction data [9].

Assignment of the ν_{OD} bands observed for $MgSO_3 \cdot 3H_2O$, β-$MnSO_3$ $3H_2O$ (at 300 and 100 K) and γ-$FeSO_3 \cdot 3H_2O$ (at 300 K) (samples deuterated by $\approx 7\%$ D) with respect to the orientation of the respective OD groups relative to the crystal axes (see Fig. 1) has been established by Raman single-crystal measurements [1,5,6,13,14]. The results are included in Fig. 6. The Raman studies further reveal that the single crystals of the $MSO_3 \cdot 3H_2O$ compounds are preserved when undergoing the phase transitions. Complete IR and Raman spectra of polycrystalline samples of the $MSO_3 \cdot 3H_2O$ compounds are given in refs. 5–7, 10 and 11.

Figure 8 shows a fit of the frequency shifts observed for the ν_{OD} bands of $MgSO_3 \cdot 3H_2O$ to a relation obtained from the Landau theory of order–disorder phase transitions [3]

$$[\nu_{OD}(T_c) - \nu_{OD}(T)]^2 \propto T$$

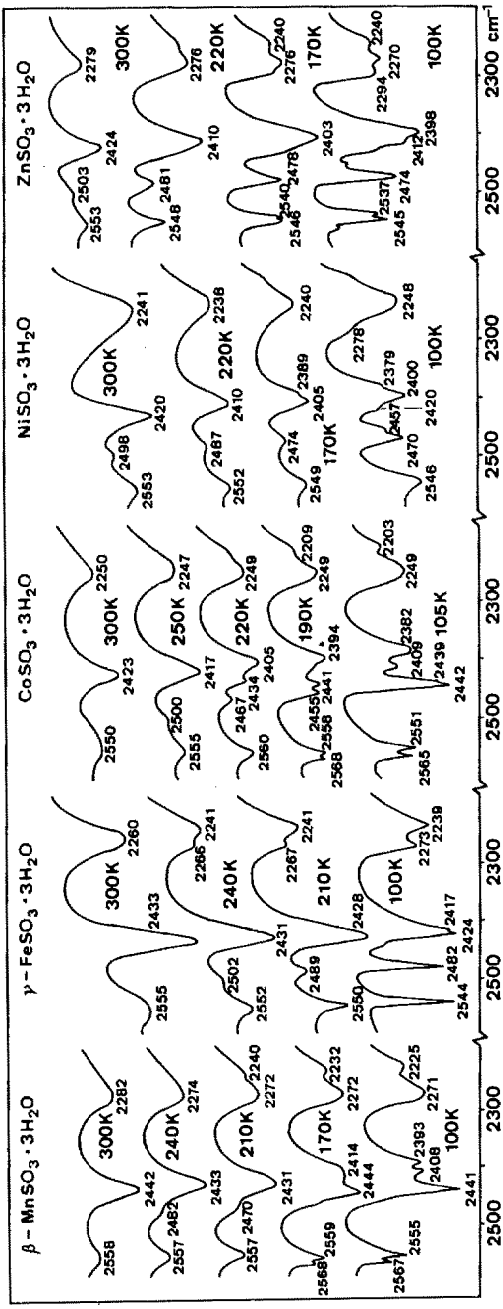

Fig. 7. IR spectra of isotopically dilute samples of isomorphic $MSO_3 \cdot 3H_2O$ in the ν_{OD} mode region at various temperatures.

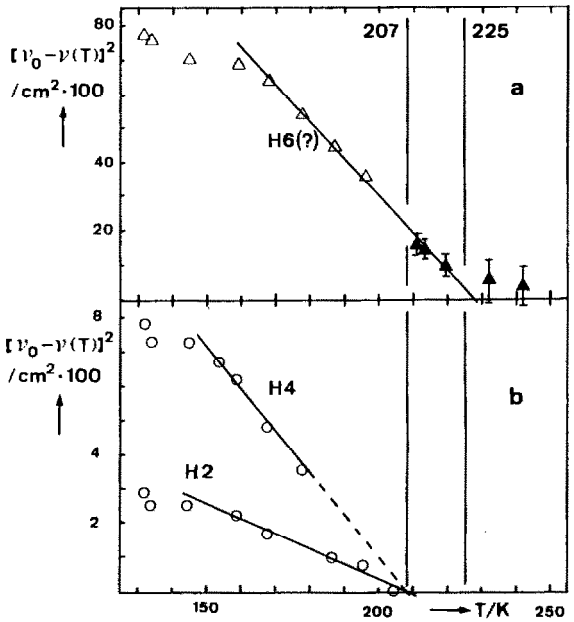

Fig. 8. Landau-like behaviour of the temperature dependence of the uncoupled OD modes of $MgSO_3 \cdot 3H_2O$ due to H_2O III at ≈ 2480 cm^{-1} (a), and H_2O I and II at ≈ 2430 (H2) and ≈ 2420 (H4) cm^{-1} (b), see Figs. 5 and 6; vertical lines, phase transitions at 207 and 225 K; $\nu_0 = 2568$ (H5, H6), 2451 (H2, H4) cm^{-1}.

From the increased halfwidth (Figs. 5, 7, and 9) of the ν_{OD} bands at ≈ 2550 cm^{-1} due to H_2O III, it can be concluded that the disorder of this water molecule is dynamic. Arrhenius plots and potential barriers derived from the linewidth data of the uncoupled ν_{OD} IR bands (H_2O III) of the magnesium,

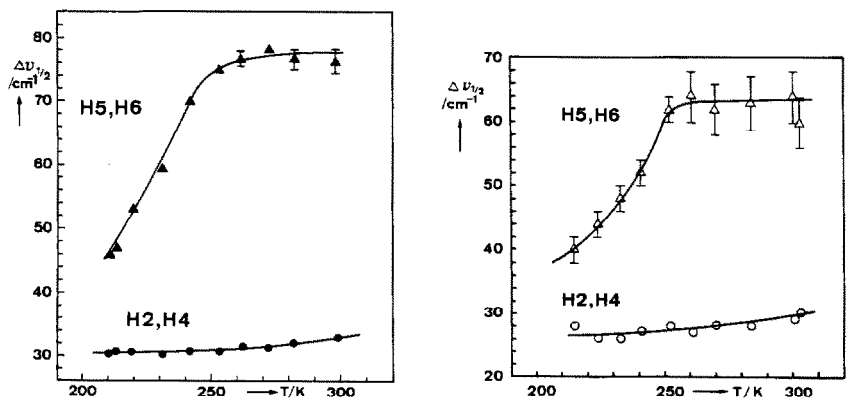

Fig. 9. Temperature shifts of the halfwidths (widths at half height) of the ν_{OD} bands due to H5 and H6 (H_2O III), and H2 and H4 (H_2O I and II), respectively, of $MgSO_3 \cdot 3H_2O$ (isotopically dilute samples); open signs, Raman spectra; filled signs, IR data.

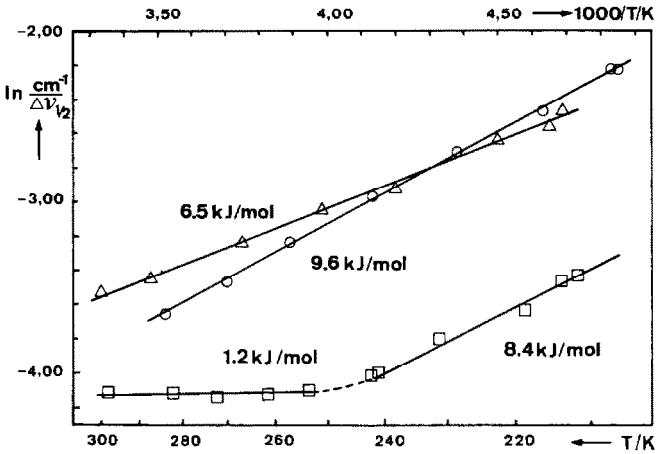

Fig. 10. Arrhenius plots ($\ln(1/\Delta\nu_{1/2})$ versus T^{-1}) of the halfwidths of the ν_{OD} IR bands due to H5 and H6 (H_2O III) of $MgSO_3 \cdot 3H_2O$ (□), β-$MnSO_3 \cdot 3H_2O$ (△) and γ-$FeSO_3 \cdot 3H_2O$ (○) (isotopically dilute samples); figures, potential barrier.

manganese and iron compounds are given in Fig. 10. The physical background of the procedure used is discussed in refs. 1, 3 and 5. At ≈ 270 K (RTM), the potential barriers, V of the reorientational motions of H_2O III increase in the order $V_{Mg} < V_{Mn} < V_{Fe}$.

DISCUSSION

The phase transition examined in this paper must be divided into two successive processes.

(i) At the higher transition temperature, i.e. at ≈ 225 K ($MgSO_3 \cdot 3H_2O$) and ≈ 235 K (β-$MnSO_3 \cdot 3H_2O$), the dynamic disorder of the H_2O III molecules starts to freeze out. This can be concluded from the frequency shifts (Figs. 5 and 9) and band narrowings (Fig. 10) of the respective ν_{OD} modes and the temperature dependence of the dielectric constant ϵ (Fig. 4). This order–disorder transition, which is not observed by X-ray methods and which obviously occurs in all of the six isomorphic $MSO_3 \cdot 3H_2O$ compounds under study, is accompanied by a strong distortion of H_2O III, namely, a splitting of the uncoupled OD modes, up to 132 cm^{-1} in the case of $MgSO_3 \cdot 3H_2O$ (see Figs. 5–8). In the case of the nickel and zinc compounds this ordering probably starts above room temperature, shown from additional ν_{OD} bands at 2498 and 2503 cm^{-1}, respectively, even at 300 K (Fig. 7).

(ii) The increasing order of H_2O III in a subsequent step then causes the small monoclinic distortion of the orthorhombic unit cell of the RTM (see Table 1), at least in the case of the sulphite trihydrates of magnesium,

manganese and cobalt. In this second transition process (at 207, 217 and 230 K), the H_2O I and II molecules, as well as the heavy atoms, are involved, as shown by the splitting of both the ν_{OD} band assigned to H4 (RTM) (Figs. 5–7) and some Bragg peaks in the Guinier photographs (Fig. 2).

For both transition steps, the frequency shifts of the respective ν_{OD} bands below the transition temperatures can be considered as order parameters (Fig. 8) and, hence, indicate that second (or higher) order mechanisms must be assumed for the transitions observed despite some results from thermoanalyses showing characteristics of first-order transition, e.g. hysteresis of the transition temperature and enthalpy effects.

The unusual isotopic effect of the phase transitions in the hydrates under discussion (Fig. 3) must be attributed to the order–disorder nature of these phase transitions. The strengths of H-bonds and D-bonds in solid hydrates differ only to a small extent [1], but there are different jump frequencies, activation energies and tunnelling probabilities due to both the different masses of H and D and to different zero point energies of the librational modes. These isotopic effects connected with the rotational motions for H_2O and D_2O molecules cause the ordering in the hydrate to occur at much higher temperatures than in the deuterohydrate or completely prevent ordering of the D_2O molecules in samples with high D content.

ACKNOWLEDGEMENTS

The authors thank Prof. Dr. H.-J. Berthold and Dipl.-Chem. G. Reiner, Hannover, for some DTA experiments, and the Deutsche Forschungsgemeinschaft and the Fonds der Chemischen Industrie for financial support.

REFERENCES

1 H.D. Lutz, Structure and Bonding, 69 (1988) 97.
2 S.K. Satija and C.H. Wang, J. Chem. Phys., 68 (1978) 4612.
3 G. Schaack, J. Mol. Struct., 79 (1982) 361.
4 J. Petzelt and V. Dvořàk, J. Phys. C: Solid State Phys., 9 (1976) 1587.
5 J. Henning, Thesis, Univ. Siegen, 1988.
6 H.D. Lutz, J. Henning, W. Buchmeier and B. Engelen, J. Raman Spectrosc., 15 (1984) 336.
7 H.D. Lutz. W. Eckers, and B. Engelen, Z. Anorg. Allg. Chem., 475 (1981) 165, and references cited therein.
8 B. Engelen, Habilitationsschrift, Univ. Siegen, 1983.
9 B. Engelen, D. Gregson, W. Gonschorek, F. Pfeiffer and H. Weitzel, Z. Kristallogr., 182 (1988) 79.
10 H.D. Lutz, S.M. El-Suradi, Ch. Mertins, and B. Engelen, Z. Naturforsch., 35b (1980) 808.

11 H.D. Lutz, S.M. El-Suradi, and B. Engelen, Z. Naturforsch., 32b (1977) 1230.
12 I. Savatinova and E. Anachkova, Phys. Status. Solidi. B: 84 (1977) 401.
13 H.D. Lutz and J. Henning, Z. Kristallogr., 178 (1987) 148.
14 J. Henning and H.D. Lutz, in R.J.H. Clark and D.A. Long (Eds.), C.R. 11th. Conf. Int. Spectrosc. Raman, 1988, 363.